

Final report of OTKA K124353

Modeling nanodevices from the atomic to the mesoscopic scale

Principal Investigator:

Dr. Dezső Boda

Professor

University of Pannonia

Center for Natural Sciences

Complex Molecular Systems Research Group

Veszprém

2017–2022

Introduction

The goal of this project was to coordinate the common efforts of the members of the Complex Molecular Systems Research Group (<https://mscms.uni-pannon.hu/>) at the Center for Natural Sciences, Faculty of Engineering, University of Pannonia to study “porous materials, in which pores, channels, cavities, slits, or other kinds of pathways make the transport, selective adsorption, or structural ordering of molecules/ions possible”.

The studied systems show complex behavior at the nanoscale resulting in useful mezoscale and macroscale behavior of the whole system considered as a device. Device behavior is characterized by the relationship of the input and output variables. We are interested in that relationship (device function) by creating models of various resolutions and by studying them with fitting statistical mechanical methods. The wide scale of the resolutions of models is the basis of the multiscale approach in which we study the core unit of the whole system in molecular detail, while the whole system is modeled by reducing certain degrees of freedom into implicit response functions.

The project was categorized into three branches supervised by the three senior researchers (D. Boda, T. Kristóf, Sz. Varga) who are experts of the respective areas and the corresponding methodologies. The report is organized accordingly.

1 Confined electrolytes: nanofluidic devices, nanopores, sensors

The systems studied by the group of **D. Boda** consist of electrolytes in a confined environment. While we were also interested in the bulk behavior of the electrolyte [37], our main interest was the behavior of ions near charged and/or chemically functionalized walls. At these walls, electrical double layers [17, 18] are formed whose structure determines the behavior of the whole device.

1.1 Multiscaling

Our studies applying the multiscaling approach followed the line started by our papers produced in the framework of our previous ERA-Chemistry OTKA grant (NN 113527) for bipolar nanopores. [7, 10] The models applied for studying nanopores and ion channels range from all-atom models including explicit water studied by molecular dynamics (MD) via reduced models using implicit water studied by Brownian Dynamics (BD) [5] or Local Equilibrium Monte Carlo (LEMC) [3] to continuum models such as Poisson–Nernst–Planck (PNP) as shown in Fig. 1.

While ionic transport is simulated directly with MD and BD, the hybrid methods combine the Nernst–Planck (NP) transport equation with statistical mechanical techniques that relate the chemical potential profile, $\mu_i(\mathbf{r})$, to the concentration profile, $c_i(\mathbf{r})$. If we combine NP with LEMC, we obtain the NP+LEMC method. [3] Dirk Gillespie combined NP with density functional theories thus obtaining a method that can be coined as NP+DFT. [1] Combining the NP equation with the Poisson–Boltzmann (PB) theory could be coined as NP+PB, but historically it was named PNP.

Our main paper on multiscaling [24] studies the effect of charge pattern on the device behavior of a nanopore. Changing the charge pattern from uniformly charged to bipolar, the pore changes

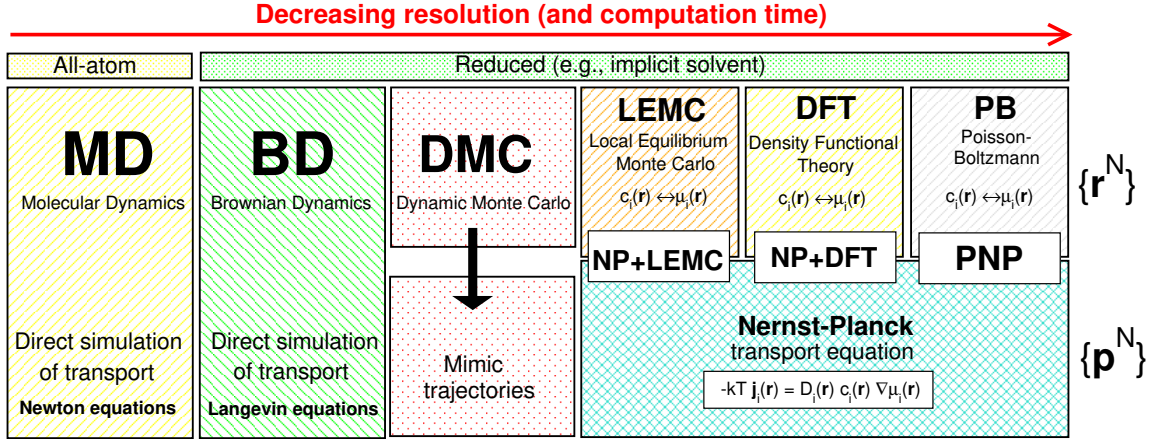


Figure 1: Models of varying resolutions and corresponding methods. [24]

from selective to rectifying. The paper also discusses how the adjustable parameter of the reduced model (the diffusion coefficient of ions inside the pore) should be chosen to be an appropriate response function. Specifically, it depends on the charge pattern, but it does not depend on voltage.

In another paper [26], we focused on the question of how to create good reduced models. We proposed four rules of thumb that emphasized the importance of appropriate reproduction of local behavior of ions resulting in a realistic behavior of the axial concentration profiles (see Fig. 2), identifying the important degrees of freedom, and choosing appropriate response functions.

Comparing the results of models of varying resolutions remained our practice in later studies [15,18,19,26,28,37,41], especially when LEMC simulations gave results that were qualitatively different from those given by the mean-field PNP (charge inversion, see subsection 1.5).

1.2 The importance of charge pattern on the pore wall

The importance of the charge pattern on the pore wall can be deduced from Fig. 2 where results for a uniformly charged pore, a bipolar pore, and a pore with a transistor-like charge pattern are shown. The uniformly charged pore is selective for the cation to a degree determined by many factors from surface charge density, σ , to electrolyte concentration, c ; more about this, see the part about scaling (subsection 1.4). [24, 41] The bipolar pore rectifies current because it is an asymmetric pore and gives fundamentally different answers for voltages of opposite signs. [7, 10, 19, 24, 28, 42] In the transistor geometry, we can control the current with the charge of the middle segment, σ_X . [15, 20]

A special case is when chemical groups are functionalized on the nanopore's surface beyond the surface charge that makes the application of nanopores as sensors possible. [9, 21, 22, 31]

1.3 Nanopore sensors

These studies followed our paper from 2017 [9] in which we created a simple model of a nanopore sensor by placing binding sites on its wall that selectively bind one ionic species, X^{z+} , with a short-range potential. The X^{z+} ions bound to the pore alter the flux of background

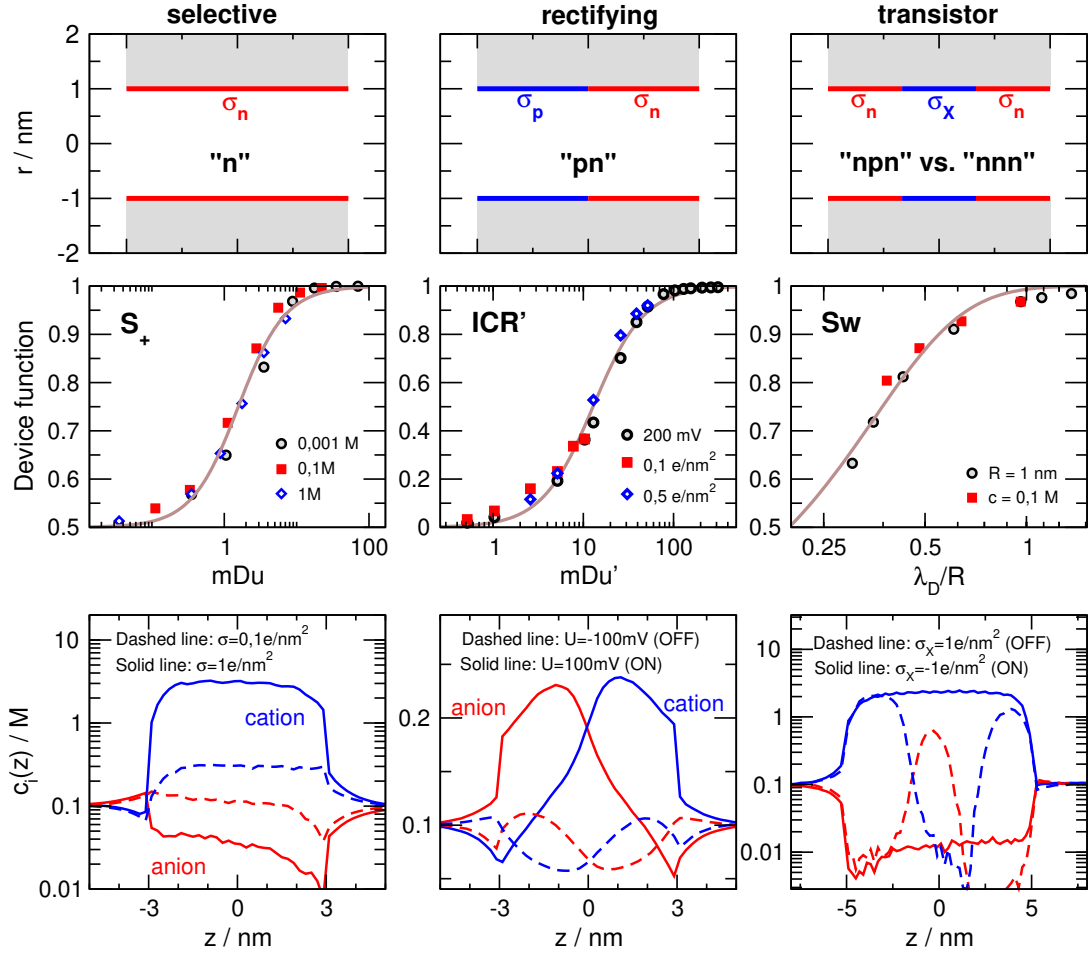


Figure 2: Different nanopores depending on the charge pattern on the wall (top row), their device functions as functions of scaling parameters (middle row), and axial concentration profiles (bottom row). [34]

cations (K^+ , for example). More X^{z+} ions exclude more K^+ , so the current depends on the $[X^{z+}]$ concentration. The analyte concentration $[X^{z+}]$ can be determined from current measurements via calibration curves.

In the present project, we were interested in the question whether we can construct nanopore sensors with different mechanisms by changing the charge pattern on its wall. After probing various charge patterns [22], we found that a bipolar nanopore is an efficient geometry with Cl^- ions being the main charge carriers. The mechanism of sensing is that more positive analyte ions attract more Cl^- ions into the pore thus increasing the current. Rectification serves as an additional device function that can be related to $[X^{z+}]$ making the device a dual-response sensor. Later, we took a closer look at the bipolar geometry. [15]

When we take pH as an additional parameter, we can tune the charge pattern on the wall of the nanopore. This gives us more freedom to design nanopore sensors according to our purposes. [31]

1.4 Scaling

Scaling and scalability are important approaches that help in understanding a nanopore's behavior in general terms. Scaling means that the function of a device is determined by a few well-defined variables, a_1, a_2, \dots via a composite parameter, ξ , that is an analytical function of the input parameters, $\xi = \xi(a_1, a_2, \dots)$, and determines the device's behavior by itself. Let F be the device function, an observable property of the device. Scaling of the device function means that F is a smooth unambiguous function of the scaling parameter: $F = f[\xi(a_1, a_2, \dots)]$.

While the first occasion we met the phenomenon was that of a nanopore sensor (currents plotted against the relative concentration $[X^+]/[K^+]$ collapsed onto each other) [9], we used the term "scaling" for the first time in our transistor study [15]. In that work, we realized that plotting the device function (switching, Sw: the ratio of currents in the OFF and ON states, see right-middle panel of Fig. 2) as a function of the λ_D/R parameter (λ_D is the Debye-length), the curves for various conditions collapse onto each other.

Later, we extended our scaling study to bipolar nanopores and proposed a scaling parameter that was valid for multivalent electrolytes as well. [19] The λ_D/R parameter controls the degree of overlap of double layers in the center of the pore. More overlapping means more efficient exclusion of coions, better selectivity, and better rectification.

Also, it was evident that scaling works better if mean-field features dominate the problem. If ionic correlations are strong, deviation from scaling appears. [28]

Recently, we paid more attention to the scaling problem more deeply and showed [41] that the Dukhin number [2]

$$\text{Du} = \frac{|\sigma|}{eRc} \quad (1)$$

is an appropriate scaling parameter for uniformly charged infinitely long nanopores (nanotube limit) where the device function is selectivity defined as

$$S_+ = \frac{I_+}{I_+ + I_-} \quad (2)$$

in the middle-left panel of Fig. 2. The mDu parameter on the abscissa is the modified Dukhin number defined as

$$\text{mDu} = \text{Du} \frac{H}{\lambda_D}, \quad (3)$$

where H is the length of the pore. This parameter proved to be a better scaling parameter for the conditions in Ref. [41] (small R , large U) because the axial effects dominate the problem over the radial effects. In that paper, we hypothesized that mDu is the good scaling parameter in the nanohole limit ($H/R \rightarrow 0$), a hypothesis that needs to be refined in the light of our recent results.

However, the axial effects naturally dominate the problem in the case of the bipolar nanopore. In that case, rectification is the device function defined as

$$\text{ICR}' = \frac{I^{\text{ON}} - I^{\text{OFF}}}{I^{\text{ON}} + I^{\text{OFF}}} \quad (4)$$

in the middle panel of Fig. 2. The mDu' parameter on the abscissa is defined as

$$\text{mDu}' = \text{mDu} \frac{U}{U_0} \quad (5)$$

that adds the voltage to the scaling parameter. [42] This scaling works for not too large voltages.

The middle row of Fig. 2 shows how scaling works in the different geometries, while the bottom row shows the behavior of axial concentration profiles that, to the first order, determine device behavior.

1.5 Charge inversion

Charge inversion appears at highly charged interfaces or localized sites in the presence of multivalent cations, because, due to strong electrostatic correlations, the cations overcharge the interface causing a rise in coions and an inversion in the sign of the electrostatic potential (zeta-potential) in the second layer. Whenever we used multivalent electrolytes in our studies and molecular simulations (LEMC), this phenomenon appeared. Examples are the anomalous behavior of rectification in bipolar nanopores [28], overcharged localized wall charges resulting in an anomalous inversion of selectivity [26], and the well-known charge inversion phenomena in electrical double layers [17].

1.6 Electrical double layers

Double layers are formed near the charged wall of the nanopore and near the membrane. If a large voltage is applied, a dipole-like positive/negative pair of double layers are formed near the two sides of the membrane due to polarization.

The structural and electrostatic properties of the double layer, however, have been in the focus of the research group for a long time. During the period of the project, we have published a systematic Monte Carlo study for the planar double layer over an extensive state space parameters of concentration, electrode charge, ionic diameters and valences. [17] This work was supplemented with a DFT study lead by our international collaborator, Dirk Gillespie. [18]

1.7 Electrorheological fluids

The research topic of the electrorheological (ER) fluids has been initiated by our colleague, István Szalai, and became an organic part of our project. We have developed a BD code to simulate transient processes in the ER fluid when the electric field is switched on. [27] Fig. 3 shows these processes as a function of time characterized by various functions such as chain length distribution, average chain length, dipole-dipole energy, diffusion constant, and correlation functions. The corresponding [video clip](#) shows the time evolution of these parameters and the formation and breaking of chains.

From these functions, characteristic times corresponding to chain formation and chain association can be deduced. [36] In a follow-up study, [35] we applied a polarizable dipole model that made it possible to compute the induced permittivity increment ($\Delta\epsilon$, the increment in addition to the Clausius–Clapeyron value). Our results are qualitatively similar to those obtained by Horvath and Szalai experimentally [4]. The electric field dependence of the induced dielectric increment revealed the same qualitative behavior that experiments did: three regions with different slopes corresponding to different aggregation processes.

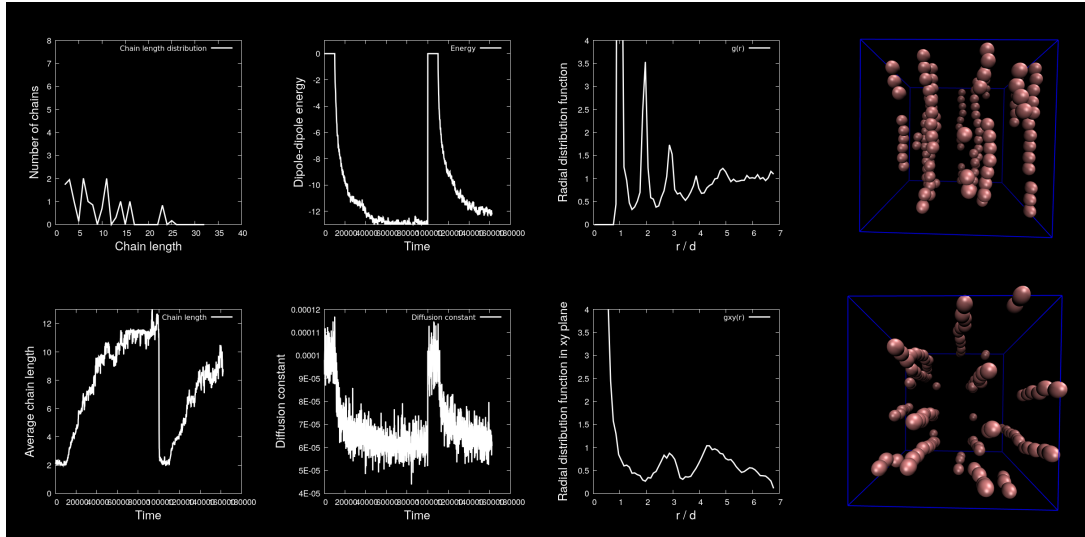


Figure 3: A snapshot of the video clip at <https://youtu.be/0wXsuz6p0W4>. [27]

2 Porous crystalline aluminosilicates

In these studies, **T. Kristóf** and his collaborators concentrated on the behavior of inorganic materials that are primarily made up of silicon (aluminum) and oxygen atoms and these atoms are linked together so that they form structurally well-defined pore systems.

2.1 Aluminosilicates with separate and regular slit pores (layered aluminosilicates)

We modeled, evaluated and compared the incorporation features of some primary intercalation reagents of kaolinite (formamide, urea and N-methylformamide) by classical molecular simulations using realistic CHARMM-based atomic force fields. Besides the determination of characteristic basal spacings of the intercalation complexes, we compared the density and orientation distributions of the guest molecules. From the simulations, we calculated the typical intermolecular interaction energies and estimated the translational mobility of the different substances. Our results show that urea has some preference over the other substances in multi-step, heat-treating intercalation/deintercalation procedures with kaolinite [14]

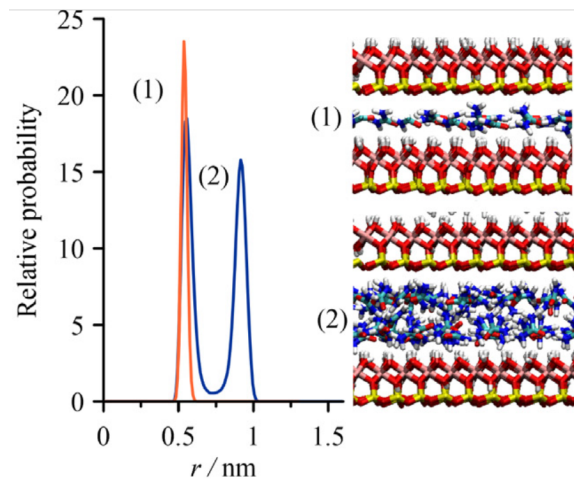


Figure 4: Kaolinite intercalation

Since kaolinite nanolayers have many important applications, it is crucial to determine the factors that govern their curling behavior. The curling of single-layer, free-standing kaolinite nanoparticles consisting of nearly 1 million atoms was studied with classical molecular dynamics simulations. The influence of force field details and of the use of different treatments of interac-

tions (long range correction, potential cut-off radius) on the curling direction were systematically examined. Both of the two possible curling directions were detected in the simulations, which contradicts the crystallographic assumption that the constituent tetrahedral sheet can exclusively be on the concave side of curled kaolinite nanolayers. The findings raise the possibility that structural changes of real-life, free-standing kaolinite nanolayers can be sensitive to small effects from the environment (intercalation reagent, exfoliation procedure), and curling in both possible directions can occur. [39]

In many environments, calcium carbonate minerals precipitate in the presence of clay minerals, and observations suggest that clays facilitate carbonate formation. In order to understand the interactions between clay surfaces and carbonate-precipitating solutions, we built model aqueous solutions (containing Ca^{2+} , Mg^{2+} and CO_3^{2-} ions) between layers of clay minerals, and performed extensive molecular dynamics simulations. Contrary to intuition, ionic clusters formed preferentially in the interlayer solution. The clusters grew both by the association of individual ions and aggregation, and were adsorbed to the clay surfaces with distinctly different efficiencies. Montmorillonite was found to be more efficient than kaolinite in capturing clusters from solution. However, the efficiency of anchoring ionic clusters to the clay surfaces depended strongly on the Na^+ concentration of the solution, since Na^+ appeared to strongly attach to the surface and thereby block it from clusters in the solution. Montmorillonite may thus have an important role in certain systems in the localization of ionic clusters on its surface, thereby promoting the nucleation of crystalline calcium-magnesium carbonate minerals. [29]

2.2 Aluminosilicates with 2D/3D interlinked pores (zeolites), where the characteristic size of the pores is similar to that of many small molecules

We made molecular simulation predictions for the adsorption of hydrogen sulphide from simple non-polar gas mixtures of technological interest (hydrodesulfurization stream outlets in petroleum refinery units) on zeolite NaA. The realistic all-atom intermolecular potential models adopted for the computations were validated by comparing the calculated isotherms of the pure substances with available experimental adsorption data. The investigated zeolite exhibited a remarkable ability to capture hydrogen sulphide, from either binary or ternary mixtures with non-polar gases (hydrogen and methane). The results suggested here that electrostatic interactions play a more pronounced role in the selective removal and the effect of molecular size has only a limited impact. [8]

The selective separation of hydrogen sulphide from industrial gas streams of light hydrocarbons by nanoporous all-silica zeolites can be an eco-friendly alternative to the other common absorption/adsorption procedures. The adsorption from binary mixtures of hydrogen sulphide and light alkanes ($\text{H}_2\text{S}/\text{CH}_4$, $\text{H}_2\text{S}/\text{C}_2\text{H}_6$, and $\text{H}_2\text{S}/\text{C}_3\text{H}_8$) on preselected all-silica zeolites was

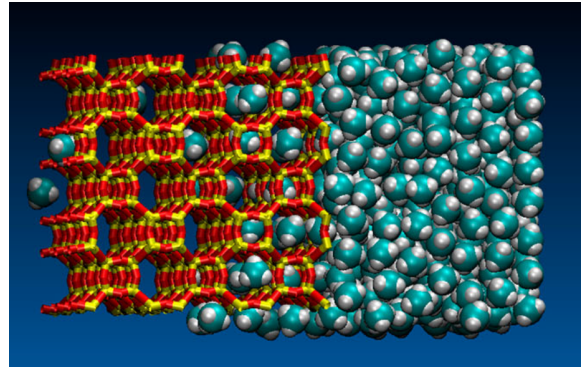


Figure 5: Zeolite adsorption

studied by atomistic simulations, using a recently developed force field for hydrogen sulphide. In addition to four experimental all-silica zeolite frameworks (DDR, CHA, ACO, CAS), three of their hypothetical relatives were also drawn into the investigations. The smaller pore size zeolites (ACO, CAS, and particularly one of the hypothetical zeolites) showed remarkable separation performances under real ambient conditions. Among the examined structural details, the calculated realistic pore size distributions proved the most appropriate in attempts to unravel the connection between adsorption selectivities and framework structural properties. [40]

3 Rod-like nanoparticles in nanoconfinement: mechanically induced ordering transitions and structural rearrangements

In this topic supervised by **Sz. Varga** the effects of planar and cylindrical confinements were studied in the systems of non-spherical hard bodies. We searched for the possibility of applying nanoconfined fluids as nanodevices and nanosensors. We examined the structural and thermodynamic properties of the following two classes of fluids:

- strictly two-dimensional fluids (2D) in bulk, slit-like pore and cylindrical pore, where the out-of-plane orientational freedom is switched off
- quasi-two dimensional fluids (q2D), where the out-of-plane orientational and the positional freedoms are switched on to some extent

We used density functional theories, replica exchange Monte Carlo simulations, and transfer operator methods for the above systems. We determined the effects of the particle's shape, the length-to-diameter ratio, and the extent of the confinement on the phase behavior of the nanofluids.

3.1 The summary of our 2D studies

It is generally accepted that the melting of 2D systems happens in two consecutive steps, where there is an intermediate mesophase between the solid and the isotropic fluid. This two-step melting can be continuous or discontinuous. The well-known prototypes of the 2D melting are 1) the discontinuous melting of the system of hard disks where the intermediate phase is hexatic, and 2) the continuous melting of hard squares where the intermediate phase is tetratic. Using the hard superdisk shape, we managed to interpolate between the melting scenario of hard disks and that of hard squares using the replica-exchange Monte Carlo simulation method. Surprisingly, we observed a new melting scenario with three steps, where there are two intermediate mesophases between the solid and the fluid phases. The resulting phase sequence is the following with decreasing the density: solid-rhombatic-hexatic-fluid (Fig. 6). The transitions between the neighboring phases are always continuous. It is new in our work that the rhombatic phase has not been observed before. In addition to this, we observed solid-to-solid transitions where the orientationally disordered solid becomes ordered with increasing density. We also detected continuous transitions between solid phases with different symmetries. [30]

We obtained exact results for the structural properties of hard spheres and hard cylinders, which are forced to stay on the surface of a cylinder. Our transfer operator method shows

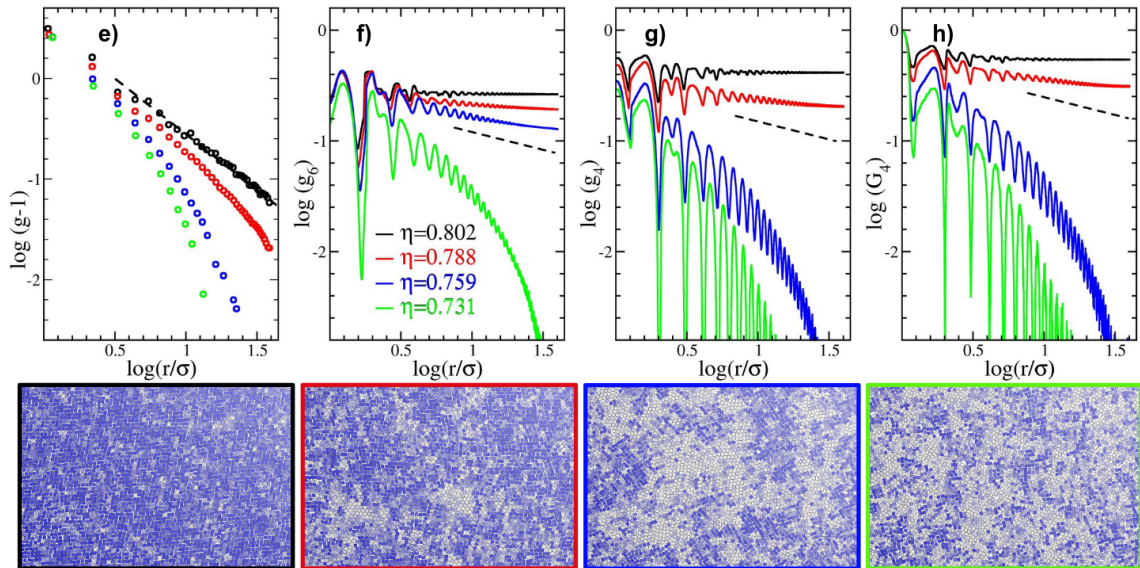


Figure 6: Panels e)-h) show the different correlation functions for various densities, η . The color of the curves matches the color of the frames of the snapshots. Particles painted blue and white are oriented parallel and forming an angle of $\pi/4$ with the snapshot director, respectively. Intermediate cases are painted with intermediate tones. [30]

that there is no possibility for phase transitions between fluid and solid structures and the close packing structure evolves continuously upon compression if only first and second neighbor interactions are present. [13]

The family of superellipse shapes is suitable to make a link between hard ellipses and hard rectangles. We determined the effects of some important molecular properties such as the particle's area and the excluded area between two superellipses on the phase behaviour of a very wide class of two-dimensional binary mixtures. With changing the deformation parameters of both components, it is possible to study several mixtures such as the superdisk–superdisk, superdisk–superellipse, superellipse–superellipse mixtures, where the shape of the superellipse is between ellipse and rectangle shapes. We managed to point out that the shape really matters in the stability of isotropic, tetratic and nematic phases using the scaled particle theory. The small rectangles proved to be the best depletion agent in the induction of strong segregation between the coexisting isotropic and nematic phases of hard ellipses. [32]

We determined the structural phase diagram of confined hard squares using replica exchange Monte Carlo simulations and density functional theories. We managed to build up a master phase diagrams where the location of different structures are shown together in a special reduced density–pore width plane. [12]

We examined the ordering properties and close packing structure of hard ellipses in confined geometries. Hard ellipses are placed between two parallel hard walls, where the ellipses form a monolayer. The effects of varying ellipse shape and the distance between the walls are studied with geometrical considerations (affine transformation) and Monte Carlo simulations. It was found that the close packing density does not depend on the shape of the ellipse, i.e., only the wall-to-wall distance determines the highest accessible density. We observed universality in the phase diagram too, where the layering transition between parallel and tilted structures in

packing fraction–pore width plane is independent from the aspect ratio of the ellipse. [33]

3.2 Summary of our q2D studies

We examined the ordering properties of non–mesogenic rod-like colloidal particles in such a narrow slit-like pore, where only one or two fluid layers are allowed to form between the two planar walls. We observed a concentration induced planar–to–homeotropic structural change and 1st order phase transitions between different structures. Our attempts to stabilize the anchoring at relatively low densities were not successful. This indicates that mechanically controlled optical switch or pressure sensor cannot be fabricated from the suspension of rod-like colloidal particles even if the particles are weakly anisotropic. [11]

The stability of uniaxial and biaxial nematic phases were examined in wider slit-like pores. It was shown that the particles tend to order parallel to the surface of the walls and wets the surface (planar wetting). As a result of the interference of density waves, which are emerging from both walls, inhomogeneous fluids with different number of layers compete with each other. The resulting phase diagram is quite complicated because uniaxial–biaxial and layering transitions are present. With increasing the density we could detect second order uniaxial–biaxial and first order phase transitions between biaxial phases at a given molecular parameters and wall-to-wall distance. We determined the global phase diagram in packing fraction–wall-to-wall distance plane for several shape anisotropies. [16]

The edge-on and face-on ordering of hard plates were examined in a narrow slit-like pore. It was found that the face-on ordering was favorable at low and intermediate densities, while the edge-on ordering occurred at high densities. We observed 1st order layering transitions between two inhomogeneous face-on fluids having n and $n + 1$ layers. We also observed that the edge-on ordering could be both uniaxial and biaxial. Even a face-on–edge-on transition can be found at high densities. [23]

The effect of out-of-plane orientational and positional freedom was examined in the system of hard spherocylinders, which were confined between two parallel hard walls. Using Onsager theory and replica exchange Monte Carlo simulation we obtained that extra particles were not needed to see isotropic–nematic phase transition with widening the pore. This means that the isotropic–nematic surface density does not change with increasing wall-to-wall distance. The stability region of the nematic phase was also widened with increasing wall-to-wall distance as the upper limit of the nematic density moved in the direction of higher densities. [25]

The stability of two-dimensional isotropic–nematic phase transition was examined in very narrow slit-like pores, where maximum two layers of fluids are allowed to form in the system of hard particles. The width of the pore was changed between the strictly 2D and the two layer forming limits for ellipsoid, spherocylinder and cylinder shapes of the particles. The naïve expectation was that we needed to insert more and more particles into the pore to induce nematic ordering, because the pore becomes more and more spacious with increasing the wall-to-wall distance. It was found that the ellipsoid shape followed this expectation as more and more ellipsoids were needed to stabilize the nematic order in wider pores. Our unexpected result was that less and less hard cylinders can stabilize the nematic phase as we made the pore more and more spacious. We found that the cross section shape of the particle is a crucial parameter

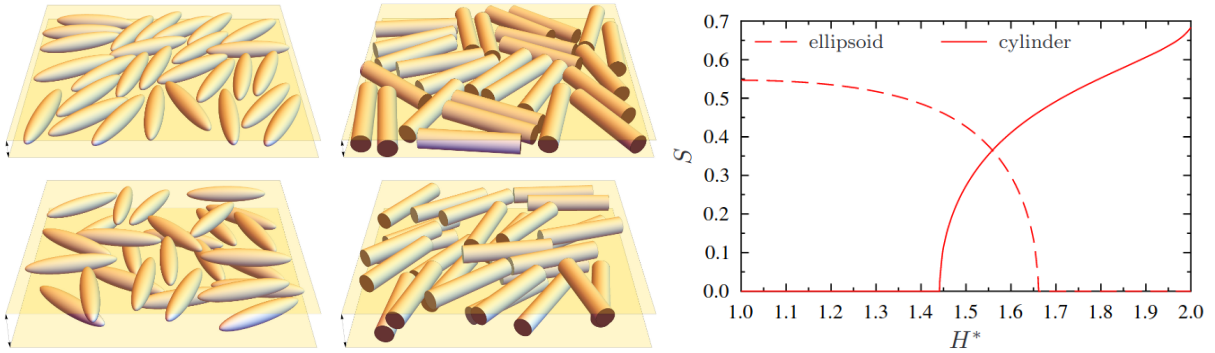


Figure 7: The effect of pore width on the nematic order (S is the order parameter) for the cases of cylinders (right) and ellipsoids (left). For video clip, see https://mscms.uni-pannon.hu/images/video/video_abstract.mp4 [38]

in the stabilization of 2D nematic ordering. The cross section of cylinder becomes needle, while that of ellipsoid collapses into a point as we go to the two-layer forming limit. [38]

Closing remarks

The project resulted in **30** papers [11–26, 28–33, 35–42] in prestigious international journals resulting in **87.4** total impact factors. We also published in Hungarian journals to strengthen our national scientific publishing. [6, 8, 27, 34] All these papers have been cited **226** times so far (**132** independent citations). The manuscripts of our papers can be downloaded from our website: <https://mscms.uni-pannon.hu/publications>

This project made it possible for [the participants](#) to focus on their studies without worrying about financial issues regarding the costs of their research. For this we owe NKFIH a debt of gratitude. We are also grateful to our international collaborators and friends, D. Gillespie, B. Matejczyk, R. Aliabadi, E. Velasco, G. Odriozola, G. Bautista-Carbajal, Y. Martínez-Ratón, H. Salehi, S. Mizani, A. Voukadinova, E. Basurto, G. Rutkai, and J. Vrabec. We also thank to our colleagues at the Faculty of Engineering for the fruitful collaborations, A. Dallos, I. Szalai, M. A. Fodor, and M. Pósfai. The role of our students (B.Sc, M.Sc, and Ph.D) cannot be overemphasized, E. Mádai, D. Fertig, Zs. Sarkadi, B. Hohl, and D. Bucsay.

References

- [1] D. Gillespie, W. Nonner, and R. S. Eisenberg. Coupling Poisson-Nernst-Planck and density functional theory to calculate ion flux. *J. Phys. Condens. Matter*, 14(46):12129–12145, 2002.
- [2] L. Bocquet and E. Charlaix. Nanofluidics, from bulk to interfaces. *Chem. Soc. Rev.*, 39(3):1073–1095, 2010.
- [3] D. Boda and D. Gillespie. Steady state electrodiffusion from the Nernst-Planck equation coupled to Local Equilibrium Monte Carlo simulations. *J. Chem. Theor. Comput.*, 8(3):824–829, 2012.
- [4] B. Horváth and I. Szalai. Structure of electrorheological fluids: A dielectric study of chain formation. *Phys. Rev. E*, 86(6):061403, 2012.

- [5] C. Berti, S. Furini, D. Gillespie, D. Boda, R. S. Eisenberg, E. Sangiorgi, and C. Fiegna. A 3-D Brownian Dynamics simulator for the study of ion permeation through membrane pores. *J. Chem. Theor. Comput.*, 10(8):2911–2926, 2014.
- [6] D. Fertig, E. Mádai, M. Valiskó, and D. Boda. Simulating ion transport with the NP+LEMC method. Applications to ion channels and nanopores. *Hung. J. Ind. Chem.*, 45(1):73–84, 2017.
- [7] Z. Ható, M. Valiskó, T. Kristóf, D. Gillespie, and D. Boda. Multiscale modeling of a rectifying bipolar nanopore: explicit-water versus implicit-water simulations. *Phys. Chem. Chem. Phys.*, 19(27):17816–17826, 2017.
- [8] T. Kristóf. Selective removal of hydrogen sulphide from industrial gas mixtures using zeolite NaA. *Hung. J. Ind. Chem.*, 45(1):9–15, 2017.
- [9] E. Mádai, M. Valiskó, A. Dallos, and D. Boda. Simulation of a model nanopore sensor: Ion competition underlines device behavior. *J. Chem. Phys.*, 147(24):244702, 2017.
- [10] B. Matejczyk, M. Valiskó, M.-T. Wolfram, J.-F. Pietschmann, and D. Boda. Multiscale modeling of a rectifying bipolar nanopore: Comparing Poisson-Nernst-Planck to Monte Carlo. *J. Chem. Phys.*, 146(12):124125, 2017.
- [11] R. Aliabadi, P. Gurin, E. Velasco, and Sz. Varga. Ordering transitions of weakly anisotropic hard rods in narrow slitlike pores. *Phys. Rev. E*, 97(1), 2018.
- [12] G. Bautista-Carbajal, P. Gurin, Sz. Varga, and G. Odriozola. Phase diagram of hard squares in slit confinement. *Sci. Rep.*, 8(1), 2018.
- [13] P. Gurin, Sz. Varga, Y. Martínez-Ratón, and E. Velasco. Positional ordering of hard adsorbate particles in tubular nanopores. *Phys. Rev. E*, 97(5), 2018.
- [14] T. Kristóf, Zs. Sarkadi, Z. Ható, and G. Rutkai. Simulation study of intercalation complexes of kaolinite with simple amides as primary intercalation reagents. *Comp. Mater. Sci.*, 143:118–125, 2018.
- [15] E. Mádai, B. Matejczyk, A. Dallos, M. Valiskó, and D. Boda. Controlling ion transport through nanopores: modeling transistor behavior. *Phys. Chem. Chem. Phys.*, 20(37):24156–24167, 2018.
- [16] H. Salehi, S. Mizani, R. Aliabadi, and Sz. Varga. Biaxial layering transition of hard rodlike particles in narrow slitlike pores. *Phys. Rev. E*, 98(3), 2018.
- [17] M. Valiskó, T. Kristóf, D. Gillespie, and D. Boda. A systematic Monte Carlo simulation study of the primitive model planar electrical double layer over an extended range of concentrations, electrode charges, cation diameters and valences. *AIP Advances*, 8(2):025320, 2018.
- [18] A. Voukadinova, M. Valiskó, and D. Gillespie. Assessing the accuracy of three classical density functional theories of the electrical double layer. *Phys. Rev. E*, 98:012116, 2018.
- [19] D. Fertig, B. Matejczyk, M. Valiskó, D. Gillespie, and D. Boda. Scaling behavior of bipolar nanopore rectification with multivalent ions. *J. Phys. Chem. C*, 123(47):28985–28996, 2019.
- [20] D. Fertig, M. Valiskó, and D. Boda. Controlling ionic current through a nanopore by tuning pH: a Local Equilibrium Monte Carlo study. *Mol. Phys.*, 117(20):2793–2801, 2019.
- [21] E. Mádai, M. Valiskó, and D. Boda. Application of a bipolar nanopore as a sensor: rectification as an additional device function. *Phys. Chem. Chem. Phys.*, 21:19772–19784, 2019.
- [22] E. Mádai, M. Valiskó, and D. Boda. The effect of the charge pattern on the applicability of a nanopore as a sensor. *J. Mol. Liq.*, 283:391–398, 2019.

- [23] S. Mizani, R. Aliabadi, H. Salehi, and Sz. Varga. Orientational ordering and layering of hard plates in narrow slitlike pores. *Phys. Rev. E*, 100(3), 2019.
- [24] M. Valiskó, B. Matejczyk, Z. Ható, T. Kristóf, E. Má dai, D. Fertig, D. Gillespie, and D. Boda. Multiscale analysis of the effect of surface charge pattern on a nanopore’s rectification and selectivity properties: from all-atom model to Poisson-Nernst-Planck. *J. Chem. Phys.*, 150(14):144703, 2019.
- [25] E. Basurto, P. Gurin, Sz. Varga, and G. Odriozola. Ordering, clustering, and wetting of hard rods in extreme confinement. *Phys. Rev. Res.*, 2(1), 2020.
- [26] D. Boda, M. Valiskó, and D. Gillespie. Modeling the device behavior of biological and synthetic nanopores with reduced models. *Entropy*, 22(11):1259, 2020.
- [27] D. Fertig, D. Boda, and I. Szalai. Brownian dynamics simulation of chain formation in electrorheological fluids. *Hung. J. Ind. Chem.*, 48(1):95–107, 2020.
- [28] D. Fertig, M. Valiskó, and D. Boda. Rectification of bipolar nanopores in multivalent electrolytes: effect of charge inversion and strong ionic correlations. *Phys. Chem. Chem. Phys.*, 22(34):19033–19045, 2020.
- [29] M. A. Fodor, Z. Ható, T. Kristóf, and M. Pósfai. The role of clay surfaces in the heterogeneous nucleation of calcite: Molecular dynamics simulations of cluster formation and attachment. *Chem. Geol.*, 538:119497, 2020.
- [30] P. Gurin, Sz. Varga, and G. Odriozola. Three-step melting of hard superdisks in two dimensions. *Phys. Rev. E*, 102(6), 2020.
- [31] B. Hohl, E. Má dai, D. Boda, and M. Valiskó. Modeling of a pH-tunable dual-response nanopore sensor. *J. Mol. Liq.*, 310:112946, 2020.
- [32] S. Mizani, P. Gurin, R. Aliabadi, H. Salehi, and Sz. Varga. Demixing and tetratic ordering in some binary mixtures of hard superellipses. *J. Chem. Phys.*, 153(3):034501, 2020.
- [33] E. Basurto, P. Gurin, Sz. Varga, and G. Odriozola. Anisotropy-independent packing of confined hard ellipses. *J. Mol. Liq.*, 333:115896, 2021.
- [34] Boda D., Valiskó M., Fertig D., Má dai E., Sarkadi Zs., Ható Z., and Kristóf T. Természetes és mesterséges nanopórusok számítógépes szimulációja. *Magyar Kémiai Folyóirat*, 127(3–4), 2021.
- [35] D. Fertig, D. Boda, and I. Szalai. Induced permittivity increment of electrorheological fluids in an applied electric field in association with chain formation: A Brownian dynamics simulation study. *Phys. Rev. E*, 103:062608, 2021.
- [36] D. Fertig, D. Boda, and I. Szalai. A systematic study of the dynamics of chain formation in electrorheological fluids. *AIP Adv.*, 11(2):025243, 2021.
- [37] D. Gillespie, M. Valiskó, and D. Boda. Electrostatic correlations in electrolytes: Contribution of screening ion interactions to the excess chemical potential. *J. Chem. Phys.*, 155(22):221102, 2021.
- [38] P. Gurin, G. Odriozola, and Sz. Varga. Enhanced two-dimensional nematic order in slit-like pores. *New J. Phys.*, 23(6):063053, 2021.
- [39] Z. Ható, J. Vrabec, and T. Kristóf. Molecular simulation study of the curling behavior of the finite free-standing kaolinite layer. *Comp. Mater. Sci.*, 186:110037, 2021.
- [40] T. Kristóf and D. Buc sai. Atomistic simulation study of the adsorptive separation of hydrogen sulphide/alkane mixtures on all-silica zeolites. *Mol. Sim.*, 48(1):31–42, 2021.

- [41] Zs. Sarkadi, D. Fertig, Z. Ható, M. Valiskó, and D. Boda. From nanotubes to nanoholes: Scaling of selectivity in uniformly charged nanopores through the Dukhin number for 1:1 electrolytes. *J. Chem. Phys.*, 154(15):154704, 2021.
- [42] D. Fertig, Zs. Sarkadi, Valiskó, and D. Boda. Scaling for rectification of bipolar nanopores as a function of a modified Dukhin number: the case of 1:1 electrolytes. *Mol. Sim.*, 48(1):43–56, 2022.